nature photonics

LETTERS

PUBLISHED ONLINE: 14 SEPTEMBER 2015 | DOI: 10.1038/NPHOTON.2015.176

# Frequency-division multiplexing in the terahertz range using a leaky-wave antenna

Nicholas J. Karl[1], Robert W. McKinney[1], Yasuaki Monnai[2], Rajind Mendis[1] and Daniel M. Mittleman[1]*

**The idea of using radiation in the 0.1–1.0 THz range as carrier waves for free-space wireless communications has attracted growing interest in recent years, due to the promise of the large available bandwidth[1,2]. Recent research has focused on system demonstrations[3,4], as well as the exploration of new components for modulation[5], beam steering[6] and polarization control[7]. However, the multiplexing and demultiplexing of terahertz signals remains an unaddressed challenge, despite the importance of such capabilities for broadband networks. Using a leaky-wave antenna based on a metal parallel-plate waveguide, we demonstrate frequency-division multiplexing and demultiplexing over more than one octave of bandwidth. We show that this device architecture offers a unique method for controlling the spectrum allocation, by variation of the waveguide plate separation. This strategy, which is distinct from those previously employed in either the microwave[8] or optical[9] regimes, enables independent control of both the centre frequency and bandwidth of multiplexed terahertz channels.**

High-bandwidth communications require the ability to multiplex and demultiplex (mux/demux) signal channels carrying independent data streams. Networks can enhance data-throughput capacity by increasing the number of non-interfering channels, which may be distinguished in a variety of ways including orbital angular momentum[10], spatial mode[11] and (most commonly) carrier frequency[12]. This latter approach has a long history, both in fibre-optic networks and in radiofrequency (RF) and microwave wireless communications for television and radio broadcasts, and more recently in mobile cellular networks.

Future wireless networks operating in the subterahertz range[1,2] will also require mux/demux capabilities. The challenges of wireless communication in this frequency range place new demands on the technologies of the physical layer. For example, transmission passbands may not be continuous, but may be segmented into multiple frequency windows due to strong frequency-dependent atmospheric attenuation from, for example, water vapour, which may also vary due to weather conditions[13,14]. Moreover, dynamic bandwidth allocation will be a crucial aspect of implementing efficient networking protocols in a terahertz network for which the transmission channels can be expected to be both bursty and highly directional[15]. As a result, it will be important to control both the channel frequencies and their bandwidths. Here, we describe a device architecture that exploits the directional nature of terahertz wireless signals to act as a free-space-to-waveguide mux/demux over a broad frequency range and which offers the flexibility to control the spectral bandwidth of each frequency channel.

Our multiplexer uses a leaky-wave antenna based on a metal parallel-plate waveguide (PPWG). Leaky-wave antennas of various types have been in use in the RF community for many years, often in the form of a metal waveguide with a narrow slot opened in one of the waveguide walls to permit some of the radiation to 'leak' out and couple to free-space modes. In the terahertz range, leaky-wave devices have not been studied in depth and only a few reports have been published to date[16–18]. Our approach relies on a PPWG in which two sides are open (thus reducing ohmic losses)[19] and where the waveguide is wide enough that the edges do not influence propagation. By opening a single slot in one of the two plates[20–23], we can allow the guided wave to leak energy into free space, or to receive energy from a free-space wave (Fig. 1).

The multiplexing principle originates from the phase-matching requirement for coupling between the waveguide mode and free

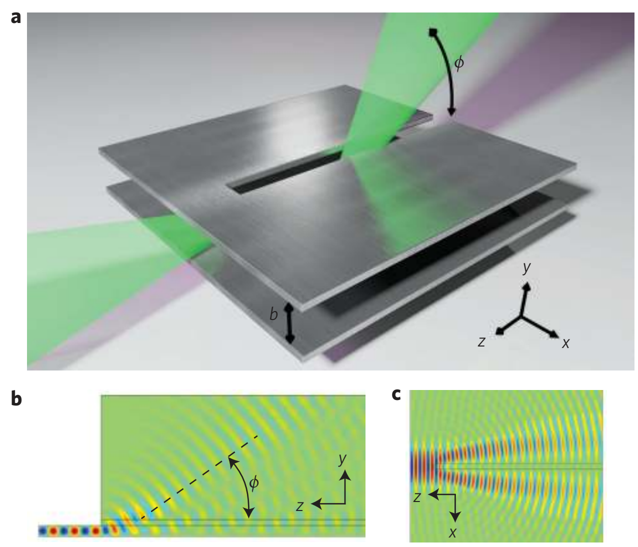


**Figure 1 | Schematic of the multiplexer. a**, A wave is coupled into a parallel-plate waveguide with plate separation $b$. This wave emerges from the leaky waveguide at a unique angle $\phi$, determined by the phase-matching condition (described in the main text). If the input wave contains multiple frequency components, then these components are demultiplexed, each emerging at a unique angle. Alternatively, in the multiplexing geometry, a wave arriving at frequency $\nu$ is coupled into the waveguide if it arrives at the correct angle $\phi$. In the experiments described here, we investigate several different values of the plate separation $b$. Other geometrical parameters include the plate thickness (1 mm), the slot length (4.2 cm), the slot width (1 mm) and the waveguide length (5 cm). **b**,**c**, Finite-element simulation of a wave emerging from the slot in a leaky waveguide. In these simulations, $b$ = 0.85 mm and the frequency is 250 GHz. A side view is shown in **b**, and a top view illustrating the wave propagating inside the waveguide is shown in **c**. These simulations show the beam emerging from the slot (thus depleting the central part of the wave inside the waveguide) and propagating into free space at the phase-matched angle $\phi$.

[1]Department of Electrical and Computer Engineering, Rice University, MS-378, 6100 Main Street, Houston, Texas 77005, USA. [2]Department of Complexity Science and Engineering, The University of Tokyo, 7-3-1 Hongo, Bunkyo-ku, Tokyo 113-8656, Japan. *e-mail: mittleman@brown.edu

NATURE PHOTONICS DOI: 10.1038/NPHOTON.2015.176

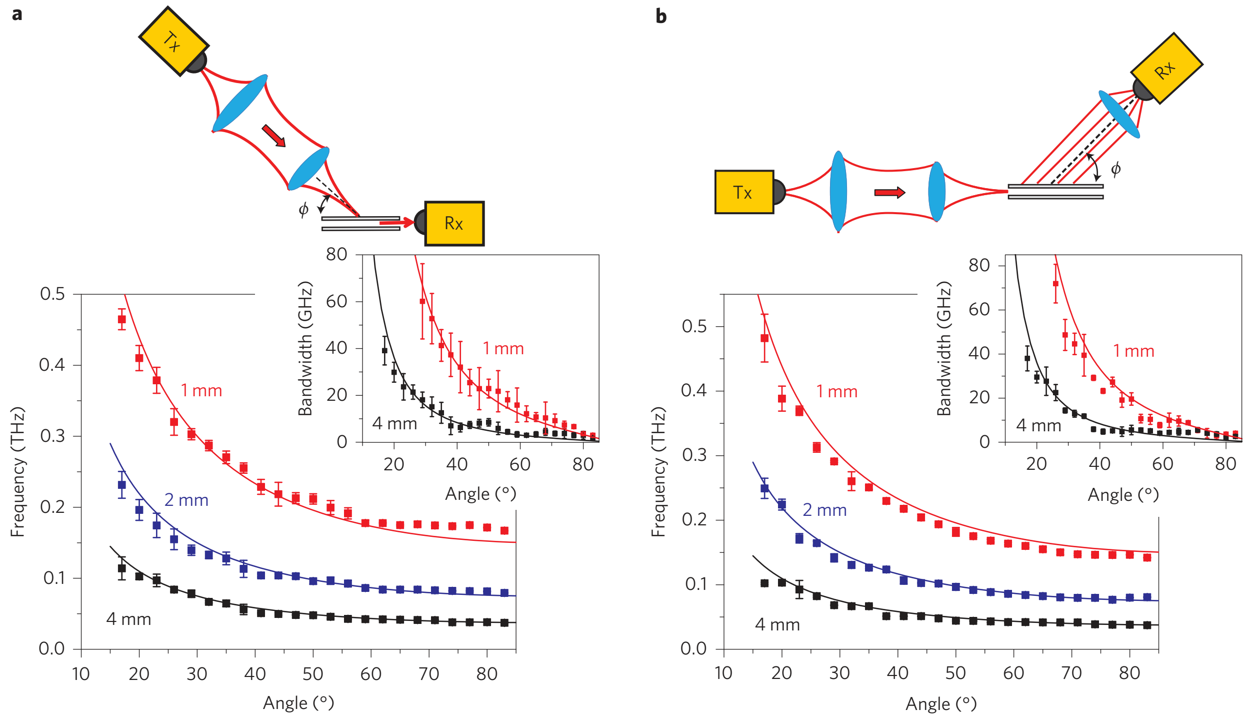


**Figure 2 | Free-space-to-waveguide coupling. a**, Measured terahertz radiation collected by the leaky waveguide when operating as a receiver (multiplexer), as a function of the angle of the incident radiation. The schematic shows the measurement set-up, with transmitter Tx mounted on a pivoting rail to vary the input angle. Results are shown for several different values of plate separation *b*. Inset: measured spectral 3 dB bandwidths at each angle. The measured results are all in good agreement with predictions (solid curves), using an acceptance aperture of $\Delta\phi = 0.25$. **b**, Similar to **a**, except here the leaky waveguide is operated as a transmitter (demultiplexer), as illustrated in the schematic. Here, receiver Rx is mounted on a pivoting rail. Error bars represent the standard error of the Gaussian-curve fit when determining the 3 dB bandwidth.

space. For the lowest-order transverse-electric ($TE_1$) mode of a PPWG, the frequency-dependent propagation constant is given by[24]

$$k_{\mathrm{PPWG}} = k_0\sqrt{1-\left(\frac{c_0}{2b\nu}\right)^2} \quad (1)$$

where $b$ is the plate separation and $k_0$ is the wavevector for free space, $k_0 = 2\pi\nu/c_0$. If the waveguide has a slot in one plate, then radiation can couple from the guided mode to free space with the phase-matching constraint that $k_0\cos\phi = k_{\mathrm{PPWG}}$. Here, $\phi$ is the propagation angle of the free-space mode relative to the waveguide propagation axis. Because of the frequency dependence of $k_{\mathrm{PPWG}}$, this condition results in an angle-dependent emission frequency:

$$\nu(\phi) = \frac{c_0}{2b\sin\phi} \quad (2)$$

Numerical simulations (Fig. 1b,c) illustrate the well-defined beam emerging from the slot and the corresponding depletion of the guided mode inside the waveguide when this phase-matching condition is fulfilled. For a given acceptance angle, $\Delta\phi$, of a receiver located in the far field of the slot, the spectral bandwidth of a given channel is described by

$$\Delta\nu(\phi) = \left|\frac{d\nu}{d\phi}\right|\Delta\phi = \frac{c_0}{2b\sin\phi\tan\phi}\Delta\phi \quad (3)$$

Conversely, when operated as a receiver, incoming free-space waves arriving at an angle $\phi$ couple into the waveguide only if they have the correct frequency, as defined by equation (2). These incoming channels will be collected with a bandwidth determined by the numerical aperture of the incoupled radiation, according to equation (3). This waveguide can therefore act as either a multiplexer or a demultiplexer between directional free-space beams and a single-mode waveguide.

We first characterize the leaky wave from a waveguide with perfectly parallel plates. The results (Fig. 2) show good agreement with equations (2) and (3) for both the transmit (demux) and receive (mux) configurations. Figure 3 shows the first experimental demonstration of the multiplexing of two terahertz input channels, using two independent broadband illumination sources and a single receiver.

Next, we consider a waveguide in which the plate separation is not constant, but varies with position inside the waveguide. This possibility provides enormous flexibility in the device design and results in new and important multiplexing capabilities. Although in this case the plates are no longer strictly parallel, we preserve single-mode propagation as long as the change in plate separation is adiabatic with respect to the wavelength[25,26].

We first study the case where $b$ varies along the waveguide propagation axis (the $z$ axis). The frequency of the incoupled channel now depends both on $\phi$ and on $z_0$, the location of the illumination point along the waveguide axis. Thus, we can achieve frequency tuning at a fixed angle, simply by translating the waveguide (and detector) relative to the input beam, along the $z$ axis (that is, varying $z_0$). We demonstrate this effect using a waveguide with two flat plates set at a 2° relative angle, so that $b(z)$ is simply a linear function of $z$ (Fig. 4).

Although it is clear that mechanical translation of the multiplexer is not a practical method for achieving high-speed frequency tuning, this result demonstrates the extra degree of freedom that can be exploited in designing a multiplexer, with input coupling optics chosen to dictate the input angle and axis for each channel. If we allow variation in both the input illumination locations and angles, we have almost arbitrary design flexibility. For example, we can design an equally spaced array of frequency bands each with

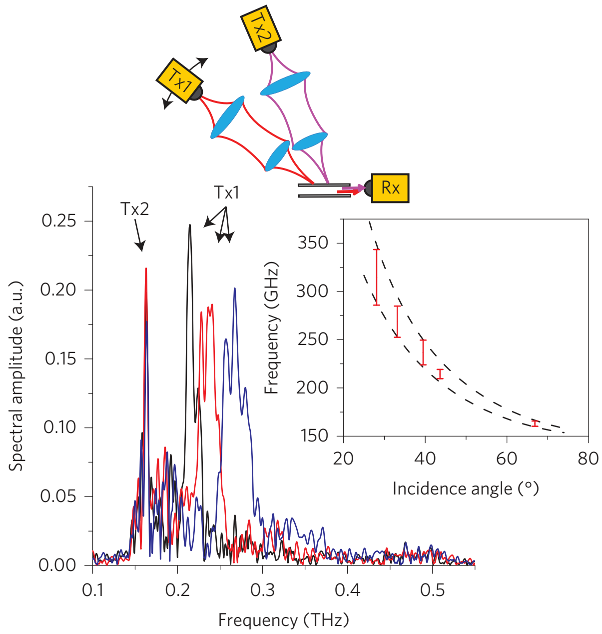


**Figure 3 | Multiplexing of terahertz signals from two transmitters.** Two different transmitters are used to illuminate the waveguide simultaneously with broadband radiation. The multiplexed signal shows two peaks with their centre frequencies determined by the input angles of the two incoupled beams, respectively. The three curves represent the results for three different angular positions of transmitter Tx1 (33.1° (blue), 39.5° (red), 43.6° (black)). In all three cases, transmitter Tx2 is fixed at $\phi = 66.9°$. Inset: the two dashed curves show the predicted spectral range versus angle, and the red bars show the measurements (in excellent agreement). To our knowledge, this is the first experimental demonstration of the multiplexing of two independent terahertz frequency channels.

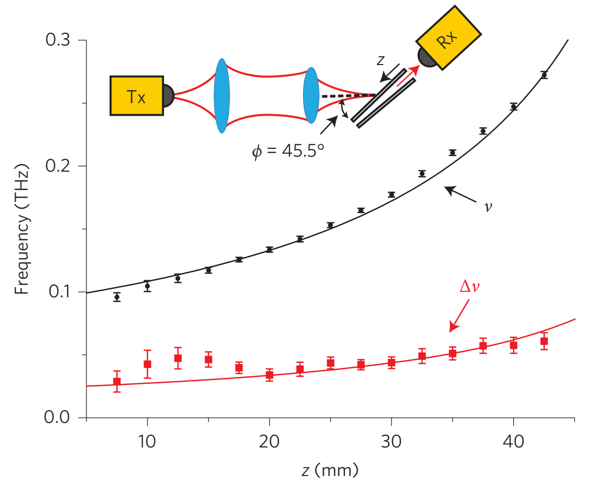


**Figure 4 | Tuning the channel frequency with plate separation.** A broadband beam illuminates the leaky waveguide at a fixed angle of 45.5°. The position of the illumination spot is translated along the $z$ axis (parallel to the upper waveguide plate) by moving the transmitter and coupling optics. Because the two waveguide plates are not parallel, the plate separation $b$ changes continuously with $z$, leading to a shift in both the frequency $\nu$ and the bandwidth $\Delta\nu$ of the detected signal. In this measurement, the plates are both flat, and the angle between the two plates is 2°, so the plate separation varies from $b = 0.5$ mm at one end of the waveguide to $b = 2.3$ mm at the other. The solid lines show the predictions of equations (2) and (3).

identical bandwidth, as is typical in fibre-based wavelength division multiplexing (WDM) systems (Supplementary Information). We have previously shown that almost any function $b(z)$ can be implemented by shaping one waveguide plate using high-resolution three-dimensional printing followed by the application of a metallic coating[26].

We next consider the case in which the plate separation $b$ varies along the transverse dimension $x$, rather than along the waveguide propagation axis $z$. At a given input angle the input coupling condition (2) can be satisfied for a range of frequencies determined by the size of the variation of $b(x)$ in the region underneath the slot. If we define the range of values of $b$ as $\Delta b$, then the range of frequencies that satisfy equation (2) is

$$\delta\nu = \frac{c_0}{2b^2 \sin\phi}\Delta b \qquad (4)$$

The bandwidth of the multiplexed channel is then determined by both the range of frequencies that satisfy the phase-matching condition and by their bandwidths, varying roughly as

$$\Delta\nu_{\text{channel}} \approx \sqrt{\Delta\nu^2 + \delta\nu^2} \qquad (5)$$

As above, $\Delta b$ could be varied by tilting the lower waveguide plate. However, a better alternative is to shape the lower waveguide plate so that the variation in $b(x)$ is symmetric with respect to the slot in the upper plate. For example, Fig. 5a illustrates a trench with cylindrical curvature, with the largest value of $b$ centred on the slot axis. This geometry has a significant advantage, in that the cylindrical curvature improves the collimation and guiding of the waveguide, by counteracting diffraction in the $x$–$z$ plane[27,28]. Using plates with several different trench depths, we demonstrate the capability for bandwidth tuning by varying $\Delta b$ (Fig. 5).

An important issue in any mux/demux design is that of losses. In our device, there are several possible sources of loss, including the coupling between free space and the waveguide mode at the input and output and the waveguide propagation loss. In our case, the propagation losses are quite small, especially for a propagation distance of only a few centimetres (for example, less than 1 dB for the experiment shown in Fig. 2)[29]. The power coupling efficiency of the $TE_1$ waveguide mode to a free-space Gaussian beam can exceed 99%[30]. Thus, the only significant source of attenuation is the coupling through the slot. In our receiver experiments (for example, Fig. 3), this coupling introduces ~9 dB of loss, due to a significant mismatch between the incoming (focusing) beam spot size and the width of the slot. However, this is far from optimized in our set-up. Significant improvements can be expected with careful design of the optical system.

In conclusion, we have investigated the radiation properties of a leaky PPWG in the terahertz range. We demonstrate mux/demux over an octave of bandwidth in the sub-terahertz range. Unlike other leaky-wave devices used for mux/demux at lower frequencies, our approach does not rely on the transparency of dielectric materials and is therefore scalable to the terahertz range. Moreover, varying the plate separation $b(x,z)$ offers a new and powerful method for controlling the frequency and bandwidth of multiplexed channels. Future designs could incorporate a variation in the width of the slot along its length, to control the leakage rate and thereby compensate for relative changes in multiplexing efficiency or in the spatial profile of different frequency channels[8]. We can also envision the implementation of an active device, based on electrostatically controlled microelectromechanical components, for dynamically varying the depth and curvature of the waveguide. Because of the large design flexibility, we anticipate that this multiplexing strategy could play a central role in future terahertz wireless systems.

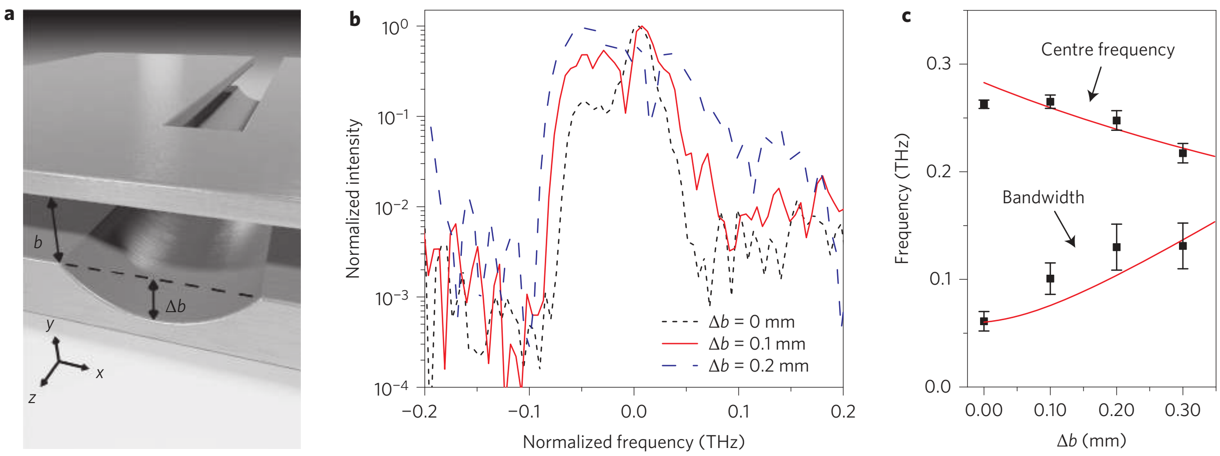


**Figure 5 | Spectrum allocation tuning with waveguide geometry. a**, Illustration of the variation in $b(x)$ provided by a cylindrically shaped trench in the lower waveguide plate, with plate separation variation $\Delta b$ as indicated. **b**, Spectra of radiation measured at the waveguide output, for several different geometrical configurations of the lower waveguide plate (that is, different values of $\Delta b$). Plate separation $b$ and the radius of curvature of the cylindrical trench are held constant, and only the trench depth $\Delta b$ is varied. To emphasize the bandwidth variation, these curves have been shifted so that their central peaks align, and are normalized to unity height. **c**, We find good agreement between the measured bandwidth of these signals, $\Delta\nu_{\text{channel}}$, and the predicted variation (solid curve) with $\Delta b$. Varying $\Delta b$ also changes the average value of $b$ underneath the slot, so the central frequency of the incoupled wave shifts slightly, as predicted.

## Methods

Methods and any associated references are available in the online version of the paper.

Received 9 February 2015; accepted 11 August 2015; published online 14 September 2015

## References


1. Piesiewicz, R. *et al.* Short-range ultra broadband terahertz communications: concepts and perspectives. *IEEE Antennas Propag. Mag.* **49,** 24–39 (2007).
2. Kleine-Ostmann, T. & Nagatsuma, T. A review on terahertz communications research. *J. Infrared Milli. Terahertz Waves* **32,** 143–171 (2011).
3. Song, H.-J. *et al.* 24 Gbit/s data transmission in 300 GHz band for future terahertz communications. *Electron. Lett.* **48,** 953–954 (2012).
4. Koenig, S. *et al.* Wireless sub-THz communication system with high data rate. *Nature Photon.* **7,** 977–981 (2013).
5. Chen, H.-T. *et al.* Active terahertz metamaterial devices. *Nature* **444,** 597–600 (2006).
6. Monnai, Y. *et al.* Terahertz beam steering and variable focusing using programmable diffraction gratings. *Opt. Express* **21,** 2347–2354 (2013).
7. Shuvaev, A. *et al.* Electric field control of terahertz polarization in a multiferroic manganite with electromagnons. *Phys. Rev. Lett.* **111,** 227201 (2013).
8. Oliner, A. A. & Jackson, D. R. in *Antenna Engineering Handbook* (ed. Volakis, J. L.) Ch. 11 (McGraw-Hill, 2007).
9. Keiser, G. *Optical Fiber Communications* 4th edn (McGraw-Hill, 2011).
10. Yan, Y. *et al.* High-capacity millimetre-wave communications with orbital angular momentum multiplexing. *Nature Commun.* **5,** 4876 (2014).
11. Luo, L.-W. *et al.* WDM-compatible mode-division multiplexing on a silicon chip. *Nature Commun.* **5,** 3069 (2014).
12. Acampora, A. S. *An Introduction to Broadband Networks* (Plenum, 1994).
13. Su, K., Moeller, L., Barat, R. B. & Federici, J. F. Experimental comparison of performance degradation from terahertz and infrared wireless links in fog. *J. Opt. Soc. Am. A* **29,** 179–184 (2012).
14. Suen, J. Y., Fang, M. T. & Lubin, P. M. Global distribution of water vapor and cloud cover—sites for high-performance THz applications. *IEEE Trans. THz Sci. Technol.* **4,** 86–100 (2014).
15. Sabharwal, A., Khoshnevis, A. & Knightly, E. Opportunistic spectral usage: bounds and a multi-band CSMA/CA protocol. *IEEE/ACM Trans. Netw.* **15,** 533–545 (2007).
16. Monnai, Y. *et al.* Terahertz beam focusing based on plasmonic waveguide scattering. *Appl. Phys. Lett.* **101,** 015116 (2012).
17. Hon, P. W. C., Liu, Z., Itoh, T. & Williams, B. S. Leaky and bound modes in terahertz metasurfaces made of transmission-line metamaterials. *J. Appl. Phys.* **113,** 033105 (2013).
18. Esquius-Morote, M., Gomez-Diaz, J. S. & Perruisseau-Carrier, J. Sinusoidally modulated graphene leaky-wave antenna for electronic beam scanning at THz. *IEEE Trans. THz Sci. Technol.* **4,** 116–122 (2014).
19. Mendis, R. & Grischkowsky, D. Undistorted guided-wave propagation of subpicosecond terahertz pulses. *Opt. Lett.* **26,** 846–848 (2001).
20. Keshavamurthy, T. L. & Butler, C. M. Characteristics of a slotted parallel-plate waveguide filled with a truncated dielectric. *IEEE Trans. Antennas Propag.* **29,** 112–117 (1981).
21. Chuang, C. W. Generalized admittance matrix for a slotted parallel-plate waveguide. *IEEE Trans. Antennas Propag.* **36,** 1227–1230 (1988).
22. Lee, C. -W. & Son, H. Periodically slotted dielectrically filled parallel-plate waveguide as a leaky-wave antenna: E-polarization case. *IEEE Trans. Antennas Propag.* **47,** 171–178 (1999).
23. Lee, J.-I., Cho, U.-H. & Cho, Y.-K. Analysis for a dielectrically filled parallel-plate waveguide with finite number of periodic slots in its upper wall as a leaky-wave antenna. *IEEE Trans. Antennas Propag.* **47,** 701–706 (1999).
24. Mendis, R. & Mittleman, D. M. A 2D artificial dielectric with $0 < n < 1$ for the terahertz region. *IEEE Trans. Microw. Theory Techn.* **58,** 1993–1998 (2010).
25. Mendis, R., Liu, J. & Mittleman, D. M. THz mirage: deflecting terahertz beams in an inhomogeneous artificial dielectric based on a parallel-plate waveguide. *Appl. Phys. Lett.* **101,** 111108 (2012).
26. Liu, J., Mendis, R. & Mittleman, D. M. A Maxwell's fish eye lens for the terahertz region. *Appl. Phys. Lett.* **103,** 031104 (2013).
27. Mbonye, M., Mendis, R. & Mittleman, D. M. Inhibiting the $TE_1$-mode diffraction losses in terahertz parallel-plate waveguides using concave plates. *Opt. Express* **20,** 27800–27809 (2012).
28. Mbonye, M., Mendis, R. & Mittleman, D. M. Measuring $TE_1$ mode losses in terahertz parallel-plate waveguides. *J. Infrared Milli. Terahertz Waves* **34,** 416–422 (2013).
29. Mendis, R. & Mittleman, D. M. Comparison of the lowest-order transverse-electric ($TE_1$) and transverse-magnetic (TEM) modes of the parallel-plate waveguide for terahertz pulse applications. *Opt. Express* **17,** 14839–14850 (2009).
30. Mendis, R. & Mittleman, D. M. An investigation of the lowest-order transverse-electric ($TE_1$) mode of the parallel-plate waveguide for THz pulse propagation. *J. Opt. Soc. Am. B* **26,** 6–13 (2009).


## Acknowledgements

The authors thank K. Reichel for contributions. This work was supported by the US National Science Foundation and the W.M. Keck Foundation.

## Author contributions

All of the authors contributed to the conception and design of these experiments. R.W.M. and N.J.K. built the set-up and collected and analysed the data. All authors contributed to the discussions and to the writing of the manuscript.

## Additional information

Supplementary information is available in the online version of the paper. Reprints and permissions information is available online at www.nature.com/reprints. Correspondence and requests for materials should be addressed to D.M.M.

## Competing financial interests

The authors declare no competing financial interests.

## Methods

All the experiments were performed using a commercial terahertz time-domain spectrometer (TDS). This is a conventional TDS system, which uses a femtosecond laser to generate and detect single-cycle terahertz pulses in lens-coupled photoconductive antennas fabricated on low-temperature-grown semiconducting substrates. These antennas were fibre-coupled for ease of repositioning. Spectra were obtained from measured time-domain waveforms via numerical Fourier transform. In these measurements, the spectral resolution was ~3 GHz, limited by the length of the optical delay line used to measure the waveforms in the time domain. The spectral content of the generated terahertz pulses exceeded 1 THz. For the angle-dependent measurements, the transmitter (or receiver) was mounted on a pivoting rail, with the pivot situated directly below the edge of the leaky-wave antenna slot, so that the angle of incidence (or emission) could be varied without changing any other geometrical parameters (for example, the propagation distance for the guided wave inside the waveguide).

The waveguides used in this study were fabricated with conventional machining of aluminium stock. We have previously determined that the surface roughness of high-quality as-purchased aluminium plates is sufficiently small that roughness losses are negligibly small at frequencies below 1 THz, even in a waveguide with a length greater than 1 m. These aluminium parts were therefore used without further modification or polishing. Machining tolerances were typically ~25 μm.